Al-Khwarizmi Engineering Journal

Al-Khwarizmi Engineering Journal
ISSN (printed): 1818 – 1171, ISSN (online): 2312 – 0789
Vol. 22, No. 1, March, (2026), pp. 14–29

Optimization of Phenol Adsorption Using Activated Carbon Derived from Spent Tea Leaves in a Packed-bed Column

Ihsan H. Dakhil [1]*, Ghazi F. Naser [2], Ahmed A. Hadi [3], and Ahmed H. Ali [4]
[1,2,4] Department of Chemical Engineering, College of Engineering, Al-Muthanna University, Al-Muthanna, Iraq
[1] College of Engineering, Al-Ayen Iraqi University, Thi-Qar, Iraq
[3] Department of Science, College of Basic Education, Al-Muthanna University, Al-Muthanna, Iraq
*Corresponding Author's Email: em2ihsan@mu.edu.iq

(Received 12 July 2025; Revised 14 December 2025; Accepted 24 December 2025; Published 1 March 2026)
https://doi.org/10.22153/kej.2026.12.011

Abstract

This study investigates the potential of spent tea leaf-derived activated carbon (STLAC) as an adsorbent for phenol removal from simulated wastewater using a packed-bed adsorber. STLAC was prepared via chemical activation through impregnation with potassium hydroxide, followed by carbonization under controlled conditions. The physicochemical characterization of the prepared activated carbon has been confirmed. Response surface methodology (RSM) with central composite design (CCD) was utilized to optimize four operating parameters: flow rate, initial phenol concentration, bed height, and pH. A quadratic mathematical model was developed to describe the relationship between these parameters and removal efficiency. Results demonstrate the high phenol removal capacity of STLAC, achieving a maximum efficiency of 91.92% under optimal operating conditions: flow rate (11.46 mL/min), initial phenol concentration (19 mg/L), bed height (17.8 cm), and pH (6.8). The first breakthrough and saturation points were observed at 31 and 70 min, respectively. Regeneration studies have confirmed the activity of STLAC for reuse in the adsorption after five cycles, with an efficiency exceeding 75%. STLAC exhibited high efficiency in phenol removal, offering advantages in terms of sustainability and cost-effectiveness. To our knowledge, this study is the first to systematically optimize phenol removal using STLAC in a continuous packed-bed column using RSM-CCD methodology and utilize the optimized parameters for determining breakthrough characteristics. This study underscores the potential of converting agricultural waste into value-added products for environmental remediation. These results demonstrate that STLAC is a promising, low-cost, and sustainable adsorbent for removing phenol from industrial wastewater.

Keywords: *Breakthrough curve; Packed-bed adsorber; Response surface methodology; Regeneration studies; Spend tea leaves; Wastewater.*

---

1. Introduction

Phenolic compounds are among the most hazardous organic pollutants found in industrial effluents from a variety of manufacturing processes, including oil refinery, pharmaceuticals, petrochemicals, plastics, paper and paints, and pesticide industries [1]. Phenol (C_6H_5OH) is the simplest type of phenolic compound. This compound belongs to a major class of toxic chemicals and poses health hazards at low concentrations due to its rapid absorption through human skin [2]. Acute or chronic exposure in humans and animals can lead to protein degradation, adversely affecting the central nervous system and potentially causing paralysis. Chronic exposure can lead to hepatic and renal damage, cardiovascular diseases, and various forms of cancer [3]. The maximum allowable concentration of phenol in drinking water is 0.002 ppm, as recommended by the Environmental Protection Agency [4]. Meanwhile, concentrations in industrial effluents can range from 35 ppm to 8000 ppm. Therefore, the efficient removal of phenol from industrial effluents before discharge into surface and groundwater is an essential environmental obligation [5].

Various treatment techniques have been developed to remove phenol. These techniques include biological treatment [6], chemical oxidation [7], ion-exchange membrane processes [8], multilayer membrane [9], photocatalytic degradation [10], advanced oxidation processes [11, 12], and adsorption [13, 14]. Among these techniques, adsorption has proven to be an effective approach for removing toxic substances from industrial wastewater [15-17], particularly suitable for treating wastewater with moderate to low pollutant concentrations, offering several advantages, such as high removal efficiency, minimal sludge production, and ease of operation [18]. Recent studies have focused on developing low-cost and efficient adsorbents to make the adsorption economical. Most studies have used agricultural wastes as adsorbents, which have been proven efficient in eliminating pollutants through adsorption [19, 20]. Recent research has focused on converting agricultural wastes into efficient adsorbent materials by enhancing their surface area and pore size through chemical activation and conversion to activated carbon. Activated carbon is widely recognized as an effective adsorbent for phenol removal due to its large surface area and porosity [21, 22]. Nevertheless, the high cost of commercial activated carbon has encouraged researchers to develop cost-effective adsorbents from agricultural waste, industrial by-products, and other natural resources [23]. Several studies have reported the preparation of activated carbon from agricultural waste [24], pistachio wood [25], cotton [26], rice husk [27], and Elm tree waste [28].

Tea is one of the widely consumed beverages worldwide, resulting in the production of large quantities of used tea leaves as waste [29]. Spent tea leaves (STLs) have attracted significant interest due to their lignocellulosic nature, wide availability, and potential as low-cost adsorbents for water treatment applications [30]. STLs are readily available, easily obtainable, and environmentally friendly and require minimal processing compared with other adsorbents. The strong adsorption performance of STLs is attributed to their porous structure and the presence of multiple functional groups, such as hydroxyl and carboxyl groups, which facilitate interactions with pollutants through hydrogen bonding, ion exchange, and physical adsorption [31, 32].

Although activated carbons derived from agricultural wastes have been extensively studied for phenol removal in batch systems, systematic optimization of continuous packed-bed column operations using response surface methodology (RSM) remains limited, particularly for STL-based materials. Furthermore, the direct application of statistically optimized conditions to determine breakthrough characteristics, a critical requirement for industrial process design, has not been reported for STLAC. To our knowledge, phenol removal in a continuous packed-bed column using activated carbon derived from STL has not been optimized using RSM methodology, and the optimized conditions have not been systematically applied to determine breakthrough curve characteristics and predict column performance. This study addresses these gaps by pursuing specific objectives, including the preparation and characterization of activated carbon derived from STLAC through chemical activation with potassium hydroxide. Thereafter, this study optimizes the influence of key operational parameters (flow rate, initial phenol concentration, bed height, and pH) on the phenol adsorption efficiency, followed by a statistical analysis of the experimental results using RSM-CCD methodology to develop a mathematical model that demonstrates the adsorption efficiency. Afterward, this study evaluates the breakthrough and exhaustion times under the optimized conditions and models the breakthrough behavior in a novel manner, as this approach has not been previously reported in the literature. Finally, regeneration studies will be conducted to reactivate the prepared activated carbon, demonstrating its efficiency for repeated use in phenol adsorption. The findings of this study will contribute to the understanding of the potential of STLAC as a sustainable biosorbent for phenol removal from industrial wastewater, providing valuable insights for the development of cost-effective treatment technologies.

2. Materials and Methods

2.1. Preparation of the Adsorbent

STLs were collected from local tea shops in Samawah, Iraq. The preparation of STLAC was conducted through several preliminary steps. First, the raw STLs were washed with tap water for 30 min to remove impurities, followed by rinsing with distilled water to eliminate suspended salts. Second, the washed leaves were dried in an oven (Memmert UF 110, Germany) at 80 °C for 24 h until a constant weight was achieved. Third, the dried tea leaves were crushed to particle sizes of 1–2 mm using a Besmak laboratory sieve shaker. This particle size range was selected based on preliminary studies, which indicated a good balance between pressure drop and mass transfer resistance. Fourth, the chemical activation step involved impregnating STLs with potassium hydroxide (KOH, 45% v/v, analytical grade, Sigma-Aldrich) at a 1:5 weight ratio (1 g STL:5 g KOH). The impregnation was carried out by mixing the STLs with the KOH solution and stirring for 2 h at room temperature to ensure uniform distribution. Fifth, the leaves were carbonized in an electric oven under nitrogen gas (99.99% purity, flow rate 150 mL/min) for 1 h at 600 °C, with a heating rate of 10 °C/min. Sixth, the prepared activated carbon was cooled to room temperature and rinsed with distilled water until the wash solution was neutralized. Finally, the neutralized STLAC was dried in an oven at 75 °C overnight and stored in a sealed glass container for later use in adsorption experiments. The carbonization temperature of 600 °C and a KOH:STL ratio of 1:5 were selected based on optimization studies by Dakhil and Ali [33], who demonstrated that these conditions maximize surface area development and pore structure formation for agricultural waste materials.

2.2. Chemicals and Reagents

Analytical-grade phenol (C_6H_5OH, 99% purity, Sigma Aldrich) was used to prepare a stock solution at 1000 mg/L concentration in double-distilled water. The desired concentrations of the different phenols were prepared by diluting the stock solution. The acidity of the test solutions was adjusted using 0.1 M hydrochloric acid (HCl, 37% purity, Merch) or 0.1 M sodium hydroxide (NaOH, 99.5% purity, Merch). Potassium hydroxide (KOH, 99% purity, Merch) used for activation was utilized without further purification. Potassium nitrate (KNO_3, 99% purity, Merk) was used for the determination of the point of zero charge.

3. Continuous Adsorption Process

The continuous flow adsorption experiments were conducted in a plastic column (PVC) with an inner diameter of 2.54 cm and a total length of 60 cm. A schematic of the experimental setup is shown in Figure 1. The column was packed with an adsorbent of STLAC between two supporting layers of glass wools (5 mm thickness each) placed at the inlet and outlet to ensure a uniform flow distribution and prevent loss of adsorbent. The packing height varies in the range 2–20 cm. The simulated phenol wastewater was prepared by diluting the stock solution to the desired concentrations in the range from 10 mg/L to 100 mg/L. The solution was introduced from a 50 L storage feed tank in an up-flow mode at flow rates of 5–25 mL/min with a peristaltic pump (Cole-Parmer Masterflex). Upward flow was selected to ensure uniform bed expansion, prevent channeling, and facilitate complete bubble removal during column packing. The flow rate was controlled using a flow meter, with excess flow recycled to the feed tank to maintain a constant concentration. The pH was set in the range of 3–9 to encompass the pHpzc of STLAC (6.4) and the pKa of phenol (9.95), allowing investigation of the protonated and ionized species interactions. The pH was measured and adjusted before each experiment with a digital pH meter (Hanna HI 2211, China) by adding drops of 0.1 M HCl or 0.1 M NaOH as needed. All experiments were carried out at room temperature (25 °C ± 2 °C). The experimental runs were designed using Box–Wilson method through RSM. The effects of the four operating factors on adsorption performance using the prepared activated carbon was investigated using a packed-bed adsorption column. Table 1 summarizes the experimental range studies. The initial and final concentrations of phenol in each experiment were measured at 500 nm with a UV-visible spectrophotometer (Shimadzu UV/Vis 1601 Spectrophotometer, Japan). A calibration curve was established in the range of 1–100 mg/L, as demonstrated in Figure 2, which shows a linear relation ($R^2 = 0.9998$). The adsorption efficiency of phenol was determined using Eq. (1).

$$Adsorption\ Efficiency(\%) = \frac{C_o - C_t}{C_o} \times 100, \ldots(1)$$

where C_o and C_t represent the initial and final phenol concentrations, measured at the beginning and end of each experiment, respectively. All experimental runs were conducted in triplicate to ensure the reproducibility of the results, and the average values were reported.

The breakthrough time (t_b) refers to the time when the concentration of the outflow reaches 5% of the concentration of the inflow ($C/C_o = 0.05$). Meanwhile, the exhaustion time (t_e) signifies the point when the outflow concentration reaches 95% of the inflow concentration ($C/C_o = 0.95$).

Table 1,
Operating parameter ranges and rationales.

Parameter	Unit	Range	Rationale
Flow rate	mL/min	5–25	To evaluate the contact time effects and mass transfer limitations
Initial phenol concentration	mg/L	10–100	Representative of the industrial effluents and to assess the driving force
Height of the bed	cm	2–20	To assess the mass transfer zone development and adsorption capacity
pH	—	3–9	To encompass pHpzc (6.4) and pKa of phenol (9.95)

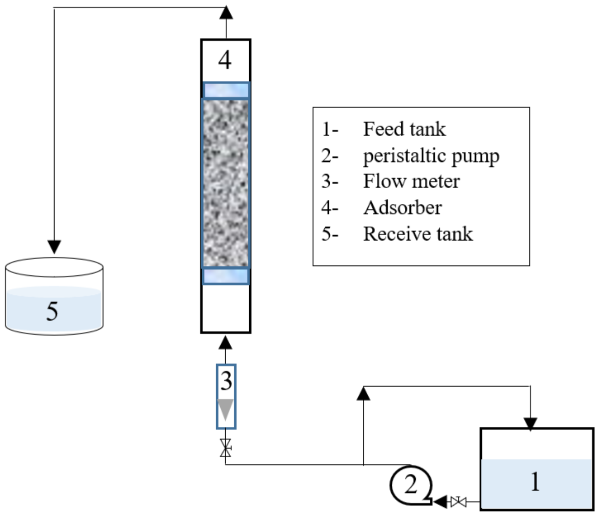

Fig. 1. Experimental work system.

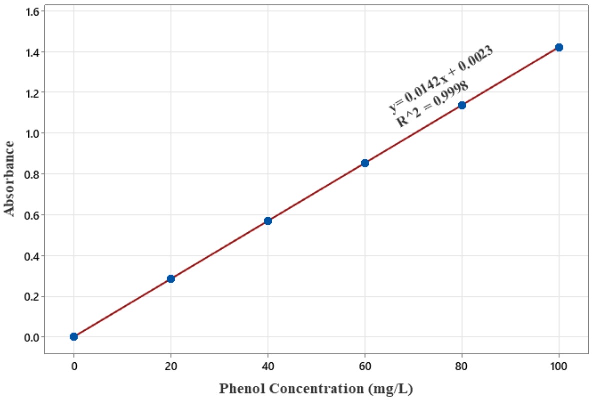

Fig. 2. Calibration curve for phenol determination.

3.1. Point of Zero Charge

The point of zero charge (pHpzc) was determined using the solid addition technique [34]. A set of 100 ml of glass beakers, each containing 45 ml of 0.01 $MKNO_3$, was prepared and adjusted to a pH value between 3 and 9. An additional KNO_3 solution was added to complete the volume to 50 mL. The initial pH value (pH_0) was measured with a digital pH meter. Approximately 1 g of the STLAC was added to each flask, which was then placed on a magnetic stirrer at a stirring rate of 120 rpm for 24 h. After filtration through Whatman No. 42 filter paper, the final pH (pH_f) was measured. The change in pH from the initial (pH_o) to final (pH_f) readings was calculated as ($\Delta pH = pH_f - pH_o$). The ΔpH values were plotted against the initial pH_o. The intercept of this curve with the x-axis (where $\Delta pH = 0$) represents the pHpzc for STLAC.

3.2. Experimental Design

The experimental runs were designed using a central composite design (CCD). This study investigated the effects of the various factors and the interaction of the operating parameters on phenol removal. Subsequently, these parameters were optimized to enhance the removal efficiency. The four tested input variables were flow rate (X_1, mL/min), initial phenol concentration (X_2, mg/L), bed height (X_3, cm), and solution pH (X_4). The dependent variable (Y, %) was the adsorption efficiency.

A five-level CCD experiment was carried out, with factorial points (coded as ±1), axial points (coded as $\pm\alpha$, where $\alpha = 2$), and center points (coded as 0). Each center point was repeated six times to determine the experimental error and confirm data reproducibility. The total number of experimental runs was 30 ($= 2^4 + 2 \times 4 + 6$), consisting of 16 factorial points, 8 axial points, and 6 center points. The coded and actual values of the independent factors are provided in Table 2.

Table 2,
Coded and actual values of the independent variables in the CCD.

Operating parameter	Unit	Variable	−2	−1	0	+1	+2
Flow rate	mL/min	X_1	5	10	15	20	25
Initial phenol concentration	mg/L	X_2	10	32.5	55	77.5	100
Height of bed	cm	X_3	2	6.5	11	15.5	20
pH		X_4	3	4.5	6	7.5	9

The experimental results were fitted to a second-order polynomial model formulated according to Eq.(2):

$$Y = \beta o + \sum \beta_i xi + \sum \beta_{ii} x_i^2 + \sum \beta_{ij} X_i X_j + \varepsilon, \ \ldots(2)$$

where Y denotes the predicted response (removal efficiency, %), βo represents the constant coefficient, β_i is the linear coefficient, β_{ii} is the quadratic coefficient, β_{ij} indicates the interaction coefficient, and ε is the error term. The model's adequacy was assessed through analysis of variance (ANOVA), with the significance of model terms determined based on p-values at a 95% confidence level (p-value less than 0.05). The precision of the model fit was assessed using the coefficient of determination (R^2), adjusted R^2, and predicted R^2. The optimal conditions were determined by solving the regression equation using the statistical Minitab-19 program and analysing the experimental results to plot the response surface in 3D representation.

3.3. Regeneration Studies

The regeneration of used STLAC was studied to evaluate its reusability over multiple adsorption–desorption cycles. After completing the adsorption experiment under optimized conditions, the column was washed with distilled water in an upward flow to remove any unadsorbed phenol. Thereafter, desorption was performed using a 0.1 M NaOH solution at a flow rate of 5 mL/min until the effluent phenol concentration was negligible. The column was rinsed with distilled water until the effluent pH reached neutrality (pH 6.5–7.5). The regenerated adsorbent was reused in the subsequently adsorption cycle. The process was repeated for five consecutive cycles. The removal efficiency in each cycle was calculated and compared to assess the regeneration efficiency. The regeneration efficiency was calculated as in Eq.(3).

$$Re\,g\,eneration\ efficiency\ (\%) = \frac{Re\,moval\ efficiency\ in\ cycle\ (n)}{Re\,moval\ efficiency\ in\ cycle\ (n-1)} \times 100 \quad \ldots(3)$$

4. Results and Discussion

The prepared STLAC was characterized, and its behavior for phenol adsorption from simulated wastewater was investigated. The factors affecting the adsorption process were studied using the packed-bed adsorption technique. Thereafter, the breakthrough point was determined based on the optimal values of the operating parameters. Afterward, the adsorbent was chemically regenerated to restore its adsorption capacity for reuse.

4.1. Physical and Chemical Properties of the Adsorbent

The elemental composition and physicochemical properties of STLAC are summarized in Table 3. The carbon content of STLAC (87.2%) is significantly higher than that of raw STL (46.8%), indicating successful carbonization of the precursor during the activation process. The hydrogen and oxygen contents decreased due to dehydration and deoxygenation reactions during pyrolysis, respectively.

The BET surface area of the prepared activated carbon is 724 m^2/g, which is relatively low compared with commercial activated carbon, which typically exhibits surface areas in the range of 900–1200 m^2/g. Despite this limitation, STLAC demonstrated considerable adsorption capacity for phenol (91.92%), suggesting that factors other than surface area, such as functional groups, pore size distribution, and chemical compound distribution on the surface, play crucial roles during adsorption.

The pore characteristics indicate that STLAC possesses a mesoporous structure (average pore diameter of 4.5 nm), which is suitable for the adsorption of organic pollutants, such as phenol. The micropore volume (0.18 cm^3/g) constitutes approximately 82% of the total pore volume, indicating substantial microporosity. The high iodine number (892 mg/g) indicates good microporosity, suggesting that the material is favorable for the adsorption of small phenol molecules. The pHpzc is 6.4 (Figure 3), indicating that the surface of the activated carbon exhibits a positive charge at pH < 6.4 and a negative charge at pH > 6.4. This property significantly influences the adsorption behavior of phenol at different pH values. The relatively low ash content (4.8%) indicates the high purity of the prepared activated carbon. The bulk density of 0.34 g/cm^3 is typical for chemically activated carbons and is suitable for packed-bed applications.

Table 3,
Characterization of STLAC.

Physical property	Value
Carbon (%)	87.2
Oxygen (%)	5.3
Nitrogen (%)	2.4
Sulfur (%)	1.5
Hydrogen (%)	0.8
BET surface area (m^2/g)	724
Total pore volume (cm^3/g)	0.22
Micropore volume (cm^3/g)	0.18
Average pore diameter (nm)	4.5
Bulk density (g/cm^3)	0.34
Moisture content (%)	5.35
Ash content (%)	4.8
Volatile matter (%)	12.3
Porosity (%)	65
Iodine number (mg/g)	892
Point of zero charge	6.4
Yield (%)	38.5

4.2. Statistical Analysis and Optimization

The experimental work for the packed bed system was designed using RSM based on a CCD to develop a mathematical model for phenol adsorption from wastewater. The levels of the operating parameters were selected based on the values that significantly affected adsorption performance in the packed column (Table 4). The experimental results were statistically analyzed using Minitab 19 to derive a quadratic mathematical model that described the adsorption efficiency, as shown in Eq.(4).

$$\text{Adsorption efficiency} = 45.7 + 0.604\,X_1 + 0.103\,X_2 + 2.969\,X_3 + 4.49\,X_4 - 0.0321\,X_1^2 - 0.001091\,X_2^2 - 0.0828\,X_3^2 - 0.356\,X_4^2 + 0.00056\,X_1X_2 - 0.0028\,X_1X_3 + 0.0250\,X_1X_4 - 0.00309\,X_2X_3 - 0.0019\,X_2X_4 + 0.0093\,X_3X_4 \quad \ldots(4)$$

The model exhibited a high correlation coefficient ($R^2 = 0.9875$) and an adjusted $R^2 = 0.9758$, indicating that 98.75% of the variability in removal efficiency is explained by the model. The predicted R^2 value of 0.9621 is in reasonable agreement with the adjusted R^2, confirming good predictive capability. The standard deviation S = 1.88%, indicating the average distance of data points from the fitted line. The acceptability and fit of the model results are verified using ANOVA, with the results summarized in Table 5. The significance of each parameter, and their interactions, is assessed at 95% confidence. Accordingly, the significant term is examined at less than 0.05 of the p-value. All the linear terms (X_1, X_2, X_3, X_4) and quadratic terms (X_1^2, X_2^2, X_3^2, X_4^2) are significant ($p < 0.05$), while none of the interaction terms are significant ($p > 0.05$), based on the p-values. The lack-of-fit p-value is >0.05, confirming that the model is adequate. The statistical analysis indicates that the operational parameters individually have a significant effect on the removal efficiency. However, the interactions of these parameters do not significantly influence the response. In addition to the data analysis, a Pareto chart is graphically illustrated using horizontal bars to illustrate the significant terms of the mathematical model at a 5% risk level, equivalent to 2.13 (Figure 4). The main significant factor is the bed height.

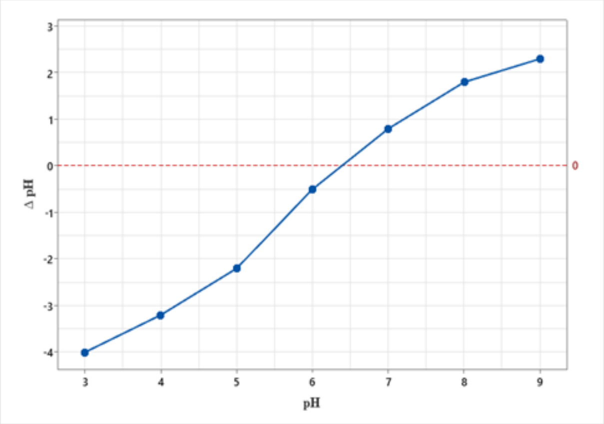

Fig. 3. Point of zero charge of STLAC.

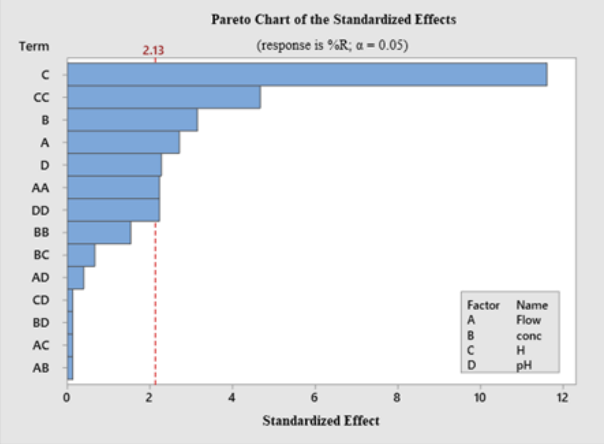

Fig. 4. Pareto chart of the standardized effects.

An optimization analysis was performed to determine the optimal operating parameter values, which provided the maximum phenol removal by a continuous packed bed. Figure 5 shows the optimal values of the operating parameters, indicated by the red vertical lines, along with the effects of these parameters on phenol adsorption. The optimal values of the operating parameters are a flow rate of 11.46 mL/min, an initial phenol concentration of 19 mg/L, a bed height of 17.8 cm, and a pH of 6.8. The maximum phenol adsorption at optimal conditions is 91.92%. The experiments conducted at the optimal operating parameter values are duplicated to confirm the achieved results.

4.3. Effect of the Operating Parameters

The effect of the four operating factors will be explained and illustrated using a surface graphical representation in three dimensions. Two factors will be changed, while the other two will remain constant at their optimal values.

Figure 6 exhibits the effect of the initial phenol concentration and solution flow rate on adsorption in a packed-bed continuous-flow column. The first enhancement in removal efficiency (from 5 mL/min to 11.46 mL/min) can be explained on the basis of mass and transfer coefficient improvement and the decrease of external film resistance. At low flow rates, the mass transfer of phenol to the external surface of the adsorbent is the controlling step. However, beyond the optimal flow rate, efficiency decreases due to the inefficient adsorbate–desorbent contact time. A residence time of 11.46 mL/min is optimal value for balancing mass transfer on external and pore surfaces. This behavior aligns with the general mass transfer zone (MTZ) theory, where excessively high flow rates cause premature breakthrough due to incomplete MTZ formation. This phenomenon is similar to the findings of adsorption of lead by rice husk [35] and phenol on modified activated carbon [36].

Table 4,
Design of the experiments using RSM.

	Coded variables				Real variables				Response
Run	X_1	X_2	X_3	X_4	Flow rate (mL/min)	Phenol conc. (mg/L)	Bed height (cm)	pH	Adsorption efficiency (%)
1	−1	−1	−1	−1	10	32.5	6.5	4.5	78
2	1	−1	−1	−1	20	32.5	6.5	4.5	76
3	−1	1	−1	−1	10	77.5	6.5	4.5	77
4	1	1	−1	−1	20	77.5	6.5	4.5	75
5	−1	−1	1	−1	10	32.5	15.5	4.5	88
6	1	−1	1	−1	20	32.5	15.5	4.5	86
7	−1	1	1	−1	10	77.5	15.5	4.5	85
8	1	1	1	−1	20	77.5	15.5	4.5	84
9	−1	−1	−1	1	10	32.5	6.5	7.5	80
10	1	−1	−1	1	20	32.5	6.5	7.5	79
11	−1	1	−1	1	10	77.5	6.5	7.5	78
12	1	1	−1	1	20	77.5	6.5	7.5	78
13	−1	−1	1	1	10	32.5	15.5	7.5	90
14	1	−1	1	1	20	32.5	15.5	7.5	89
15	−1	1	1	1	10	77.5	15.5	7.5	88
16	1	1	1	1	20	77.5	15.5	7.5	86
17	0	0	0	0	15	55	11	6	87
18	0	0	0	0	15	55	11	6	88
19	0	0	0	0	15	55	11	6	87

	Coded variables				**Real variables**				**Response**
Run	**X_1**	**X_2**	**X_3**	**X_4**	**Flow rate (mL/min)**	**Phenol conc. (mg/L)**	**Bed height (cm)**	**pH**	**Adsorption efficiency (%)**
20	0	0	0	0	15	55	11	6	86
21	−2	0	0	0	5	55	11	6	89
22	2	0	0	0	25	55	11	6	82
23	0	−2	0	0	15	10	11	6	90
24	0	2	0	0	15	100	11	6	83
25	0	0	−2	0	15	55	2	6	74
26	0	0	2	0	15	55	20	6	90
27	0	0	0	−2	15	55	11	3	85
28	0	0	0	2	15	55	11	9	86
29	0	0	0	0	15	55	11	6	87
30	0	0	0	0	15	55	11	6	87

Table 5,
ANOVA for the phenol adsorption model.

Source	**DF**	**Adj SS**	**Adj MS**	**F-Value**	**p-Value**	**Effect**
Model	14	652.783	46.627	13.18	0.000	
Linear	4	556.500	139.125	39.31	0.000	
Flow rate (X_1)	1	26.042	26.042	7.36	0.016	S
Initial conc. (X_2)	1	35.042	35.042	9.90	0.007	S
Bed height (X_3)	1	477.042	477.042	134.80	0.000	S
pH (X_4)	1	18.375	18.375	5.19	0.038	S
Square	4	93.908	23.477	6.63	0.003	S
X_1^2	1	17.646	17.646	4.99	0.041	S
X_2^2	1	8.360	8.360	2.36	0.145	NS
X_3^2	1	77.146	77.146	21.80	0.000	S
X_4^2	1	17.646	17.646	4.99	0.041	S
Two-way interaction	6	2.375	0.396	0.11	0.994	NS
X_1X_2	1	0.062	0.062	0.02	0.896	NS
X_1X_3	1	0.062	0.062	0.02	0.896	NS
X_1X_4	1	0.563	0.563	0.16	0.696	NS
X_2X_3	1	1.562	1.562	0.44	0.516	NS
X_2X_4	1	0.063	0.063	0.02	0.896	NS
X_3X_4	1	0.063	0.063	0.02	0.896	NS
Error	15	53.083	3.539			
Lack-of-fit	10	53.083	5.308			

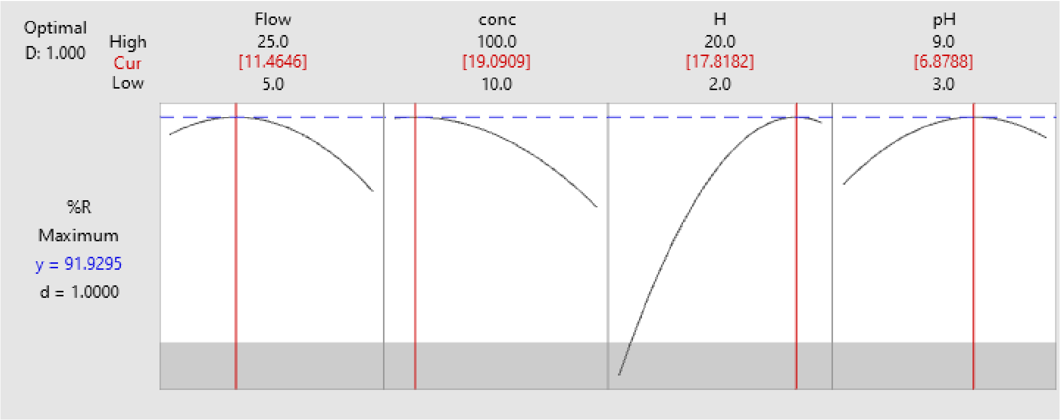

Fig. 5. Optimal values of the operating parameters.

The influence of the flow rate and bed height on adsorption is presented in the packed bed column for the constant inlet and initial phenol and pH concentrations, and the optimal process conditions are equal to 19 mg/L and 6.8, respectively (Figure 7). The findings confirmed that the adsorption capacity rises with increasing bed height, due to an increase in the adsorbent media volume, which in turn increases the vacant positions on the STLAC surface. The maximum adsorption efficiency occurred at a height of 17.8 cm in the bed. This result is consistent with almost all studies, such as phosphorus removal on rice husk [37] and nickel adsorption using activated carbon [38].

Figure 8 exhibits the influence of flow rate and pH on adsorption in a packed bed column, with the initial phenol concentration and bed depth fixed at optimized levels of 19 mg/L and 17.8 cm, respectively. The removal efficiency is pH-dependent, likely due to the competition between the adsorbent surface charge and phenol speciation. At pH < pHpzc (6.4), the surface of STLAC is protonated (positively charged). However, at pH > 6.4, the STLAC becomes deprotonated (negatively charged). Phenol has a pKa of 9.95 and exists primarily in its molecular form below pH 10. Above this pH, phenol predominantly occurs as the phenolate anion ($C_6H_5O^-$). At a pH as low as three, over-protonation results in electrostatic repulsion between the H-enriched protonated phenol species. Meanwhile, the high concentration of H^+ competes with surface adsorption sites. These effects decrease as pH comes close to the optimal value (6.87). At pH 6.87 (close to but above pHpzc), the surface is negatively charged, and phenol is mostly molecular. Consequently, different adsorption events are expected. Although the electrostatic attraction at pH >7.5 can promote the adsorption of molecular phenol onto negatively charged surface sites, increasing OH^- concentrations can result in competitive adsorption. Moreover, near the pKa, the ionization of phenol to phenolate is increased and can be traversed due to the repulsion from the negative surface. This mechanistic interpretation is supported by the observed adsorption energy, indicating that physical adsorption dominates; this finding is consistent with phenol onto sawdust, wherein a similar pH optima has been reported [39].

Figure 9 demonstrates the combined influence of these variables to comprehensively evaluate the interaction between two operating parameters. When the curves in the figure are parallel, it indicates no mutual influence, whereas non-parallel curves signify interaction between the factors. A significant angle between the curves indicates a substantial interaction. The graphical representation in this figure illustrates how four operating parameters affect phenol removal efficiency, indicating that these factors do not interact with one another.

4.4. Breakthrough Curve

The concluded optimal values of the operating parameters were used to determine the breakthrough curve for phenol adsorption. The operating factors were fixed at optimal values to plot the breakthrough curve. Several samples were collected at various time intervals, and the corresponding C/C_o values were plotted as a function of time in the form of a breakthrough curve (Figure 10). The breakthrough time (t_b) (C/C_o = 0.05) of the breakthrough curve was detected at 31 min. Meanwhile, the saturation points of exhaust time (t_e) (C/C_o= 0.95) was detected at 70 min. These results demonstrate a rapid adsorption in the continuous mode for the phenol removal from wastewater, which is superior to previous studies in the literature. These findings support the effectiveness of activated carbon in removing phenol from wastewater. Table 6 presents a comparison of the activated carbon derived from agricultural waste for phenol removal, as reported in the literature, with the findings of this study.

Table 6,
Comparison of activated carbon breakthrough and exhaust times for phenol removal.

Adsorbent	Particle diameter	Activation method	Bed height (cm)	Breakthrough time (min)	Exhaust time (min)	Removal (%)	Regeneration (%)	Reference
Date stones	2	H_3PO_4	20	25	216	85	68	[40]
Olive stone	1.5–3	$ZnCl_2$	15	48	150	88	72	[41]
Corn cob	0.3–0.8	Physical	10	180–240	480-720	85	58	[42]
Lantana camara	1–2	KOH	5–15	120–360	360–750	82	62	[43]

Rice husk	0.5–1.0	H_2SO_4	8–15	150–420	720–1440	82	65	[44]
Date stone	0.225–1.47	$ZnCl_2$	10–20	300–600	420–780	89	65	[45]
Sugarcane Bagasse	0.8–1.2	KOH	12–25	240–480	600–1200	79	70	[46]
Commercial AC	1–2	Thermal	15	20–360	60–600	85–98	75–80	[47]
Spent tea leaves	1–2	KOH	17.8	31	70	91.92	76.7	This study

4.5. Regeneration Studies

The regeneration and reusability of the STLAC adsorbent were evaluated by conducting five consecutive adsorption–desorption cycles under the optimal conditions. Figure 11 shows the removal efficiency in each cycle. The removal efficiency slightly decreased from 88.4% at the first cycle to 76.7% at the fifth cycle, representing a 15.22% reduction over five cycles. This reduction in removal efficiency can be due to several factors, including incomplete phenol desorption and structural changes on the adsorbent during the desorption. Meanwhile, some adsorption sites are blocked by the irreversible adsorption of phenol molecules. The sodium hydroxide concentration (0.1 M NaOH) for phenol desorption can result in partial hydrolysis of the functional groups on the surface, which will diminish the adsorption capacity in the regeneration cycles. Despite the gradual decrease, the removal efficiency remained above 75% after five cycles of operation, demonstrating that STLAC can be reusable multiple times in a practical process.

The regeneration efficiency (removal efficiency in a given cycle relative to that in the first cycle) is as high as 76.7%after five cycles of use, which can be considered reasonable for practical applications. The reuse of the regenerated adsorbent is important to assess its economic feasibility for industrial applications. The satisfactory regeneration efficiency of STLAC, along with its low production cost, makes it a promising adsorbent for sustainable wastewater treatment.

The regeneration ability of STLAC is proven to be superior to other agricultural waste-based ACs using similar chemical regeneration. The performance is particularly notable when using 0.1 M NaOH at room temperature, compared with thermal regeneration at 400 °C, which consumes a significant amount of energy.

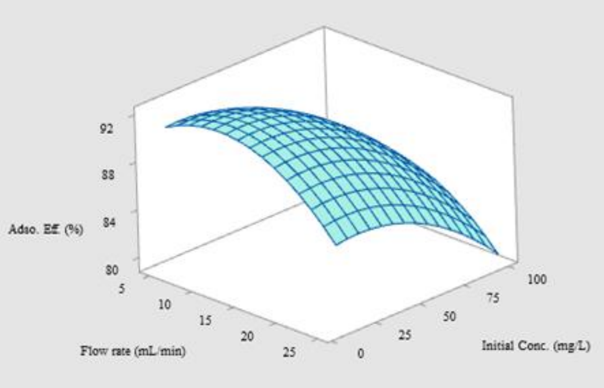

Fig. 6. Effect of flow rate versus initial concentration at the optimal values of the bed height and pH.

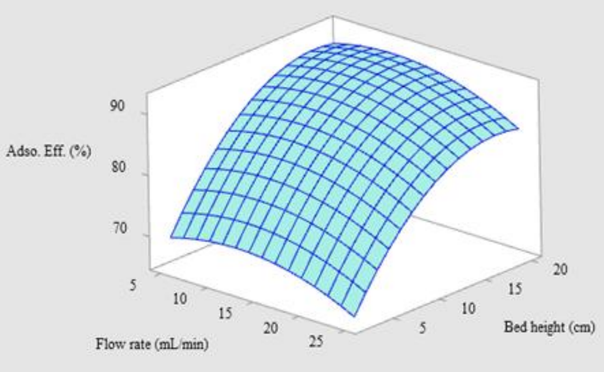

Fig. 7. Effect of flow rate versus bed height at the optimal values of the initial concentrations and pH.

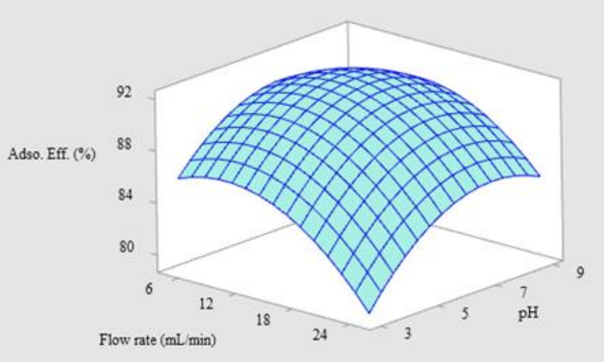

Fig. 8. Effect of flow rate versus pH at the optimal values of the initial concentration and bed height.

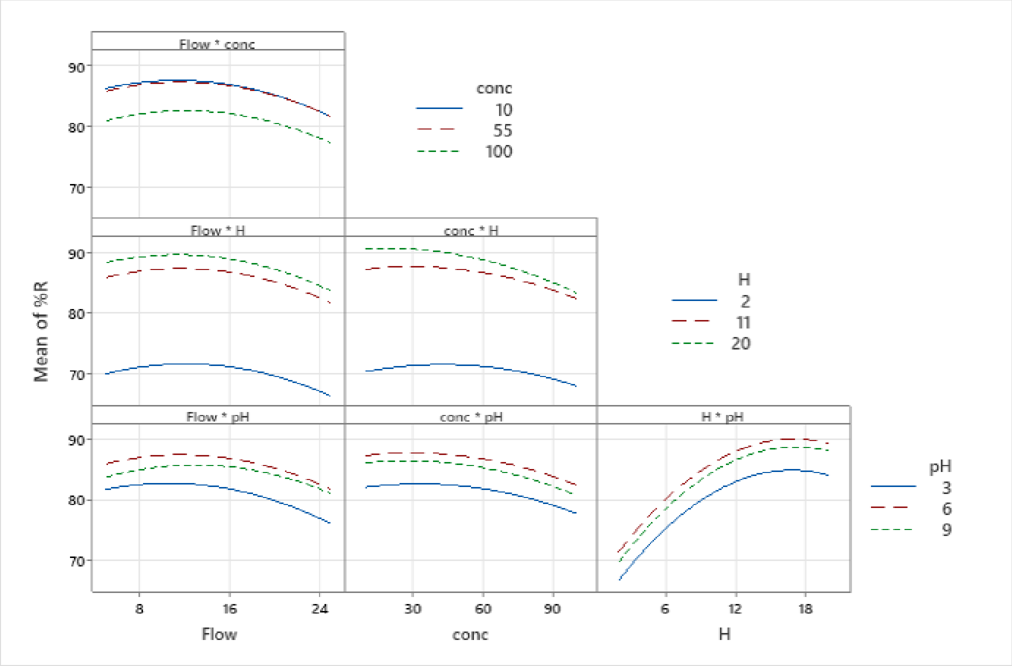

Fig. 9. Interaction of the operating factors.

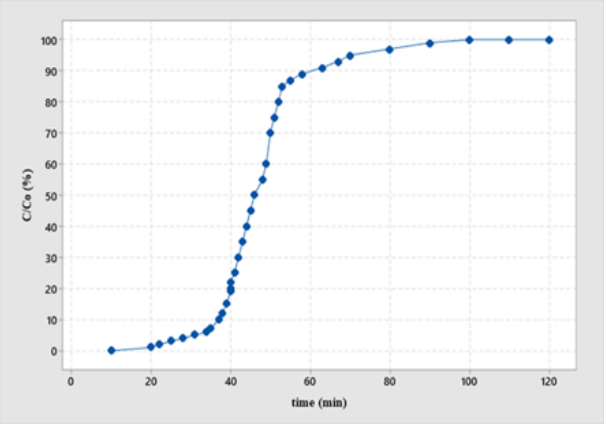

Fig. 10. Breakthrough curve.

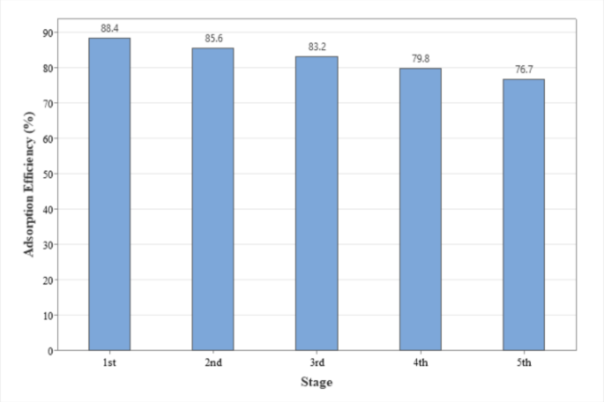

Fig. 11. Regeneration studies for the phenol adsorption on STLAC.

5. Conclusions

This study effectively demonstrated the potential of STLAC as an affordable and sustainable adsorbent for the continuous removal of phenol from industrial wastewater. The removal efficiency of 91.92% is achieved under the optimal operating parameters (11.46 mL/min flow rate, 19 mg/L initial concentration, 17.8 cm bed height, and 6.8 pH) through RSM optimization. Meanwhile, the developed quadratic model (R^2 = 0.9875) showed good predictive strength, as confirmed by the statistical analysis.

The novelty of this study lies in combining RSM-based optimization with breakthrough curve design, which enabled the identification of critical operational points: breakthrough at 31 min and exhaustion at 70 min, both demonstrating significantly faster kinetics than those reported for other agricultural waste-based adsorbents. Mechanistic studies have demonstrated that the π–π sandwich effect, hydrogen bond formation, and pore filling effects collectively contributed to the high adsorption efficiency, despite moderate specific surface areas, by leveraging the mesopore structure for a rapid mass transfer.

The regeneration tests up to five cycles indicated stable performance (76.7%). This reusability, along with waste feedstock abundance, makes this material a competitive candidate compared with costly commercial AC for industrial wastewater treatment. However, several limitations warrant acknowledgment. The investigation is suitable at the laboratory scale (bed height of 17.8 cm) under controlled conditions. Nonetheless, validation at the pilot scale is necessary to account for the great complexity of industrial wastewaters. The relatively low bed utilization indicates opportunities for improvement through staged column arrangements or pulsed-flow operation. Furthermore, adsorbent durability beyond five cycles and a techno-economic analysis comparing the production cost compared with commercial AC have not been fully addressed.

Conflict of Interest

The authors declare no conflict of interest in the publication of this paper.

References

[1] G. Escobedo-Morales, J. U. Hernández-Beltrán, N. Balagurusamy, A. Y. Hernández-Almanza, and M. P. Luévanos-Escareño, "Immobilized enzymes and cell systems: an approach to the removal of phenol and the challenges to incorporate nanoparticle-based technology," *World Journal of Microbiology and Biotechnology,* vol. 38, no. 3, pp. 1-20, 2022. https://doi.org/10.1007/s11274-022-03229-0

[2] Y. Zhang, P. Cai, G. Cheng, and Y. Zhang, "A brief review of phenolic compounds identified from plants: Their extraction, analysis, and biological activity," vol. 17, no. 1, p. 1934578X211069721, 2022. https://doi.org/10.1007/s00217-022-04163-z

[3] T. Murai and S. Matsuda, "The Chemopreventive Effects of Chlorogenic Acids, Phenolic Compounds in Coffee, against Inflammation, Cancer, and Neurological Diseases," *Molecules,* vol. 28, no. 5, p. 2381, 2023. https://doi.org/10.3390/molecules28052381

[4] O. B. Otitoju, M. O. Alfred, O. O. Ogunlaja, C. G. Olorunnisola, O. D. Olukanni, A. Ogunlaja, M. O. Omorogie, and E. I. Unuabonah, "Pollution and risk assessment of phenolic compounds in drinking water sources from South-Western Nigeria," *Environmental Science and Pollution Research,* vol. 30, no. 31, pp. 76798-76817, 2023. https://doi.org/10.1007/s11356-023-27622-w

[5] K. Grace Pavithra, P. Sundar Rajan, J. Arun, K. Brindhadevi, Q. Hoang Le, and A. Pugazhendhi, "A review on recent advancements in extraction, removal and recovery of phenols from phenolic wastewater: Challenges and future outlook," *Environmental Research,* vol. 237, p. 117005, 2023. https://doi.org/10.1016/j.envres.2023.117005

[6] X. An, Y. Wang, C. Yu, and X. Hu, "Biochar-bacteria coupling system enhanced the bioremediation of phenol wastewater-based on life cycle assessment and environmental safety analysis," *Journal of Hazardous Materials,* vol. 480, p. 136414, 2024. https://doi.org/10.1016/j.jhazmat.2024.136414

[7] H. Xu, X. Sun, H. Yang, J. Cui, J. Wang, Y. Kang, J. Deng, and G. Huang, "Degradation of aqueous phenol by combined ultraviolet and electrochemical oxidation treatment," *Journal of Cleaner Production,* vol. 436, p. 140672, 2024. https://doi.org/10.1016/j.jclepro.2024.140672

[8] S. K. Al-Amshawee, M. Y. Yunus, and I. H. , "Ion exchange membrane electrodialysis for water and wastewater processing: application of ladder-type membrane spacers to impact solution concentration and flow dynamics," *Environmental Science and Pollution Research,* pp. 1-22, 2023. https://doi.org/10.1007/s11356-023-27940-z

[9] S. K. A. Al-Amshawee, M. Y. Bin Mohd Yunus, and I. Habib Dakhil, "Multilayered membrane spacer: does it enhance solution mixing?," *Journal of Chemical Technology & Biotechnology,* vol. 98, no. 11, pp. 2627-2638, 2023. https://doi.org/10.1002/jctb.7344

[10] A. Al-Nayili and W. A. Alhaidry, "Batch to continuous photocatalytic degradation of phenol using nitrogen-rich g-C3N4 nanocomposites," *Research on Chemical Intermediates,* vol. 49, no. 10, pp. 4239-4255, 2023. https://doi.org/10.1007/s11164-023-05099-z

[11] I. H. Dakhil and A. S. Abbas, "Preparation, characterization, and performance of potential stainless steel electrodes modified with immobilized semiconductors for persistent organic pollutants via photoelectro-Fenton process," *Clean Technologies and Environmental Policy,* 2025. https://doi.org/10.1007/s10098-025-03334-2

[12] G. F. Naser, I. H. Dakhil, and A. A. Hasan, "Evaluation of electro-fenton process for removal of amoxicillin from simulated wastewater," *Global NEST Journal,* vol. 26, pp. 1-6, 2024. https://doi.org/10.30955/gnj.006075

[13] I. A. Taher, Dakhil, I.H., Kubba, Ziyad, Ali, Ahmed Hassan, "Degradation High Concentration of Eosin Yellowish Dye in Heterogeneous Catalyst Solution," *Journal of Global Pharma Technology,* vol. 10, no. 11, pp. 704-709, 2018. http://jgpt.co.in/index.php/jgpt/article/view/1900

[14] A. H. Ali, Dakhil, I. H., "Photocatalytic decolorization of Methyl Red dye under solar light," *Jornal of kerbala university,* vol. 10, no. 3, 2012.

[15] I. H. Dakhil, "Adsorption of Chromium (VI) from Aqueous Solutions using Low Cost Adsorbent: Equilibrium and Regeneration Studies," *Journal of Engineering,* vol. 19, no. 11, pp. 1395-1407, 2013. https://doi.org/10.31026/j.eng.2013.11.04

[16] I. H. Dakhil, "Adsorption of Lead from Industrial Effluents using Rice Husk," *International Journal of Engineering and Management Research (IJEMR),* vol. 5, no. 1, pp. 109-116, 2015.

[17] I. H. Dakhil, "Removal of Kerosene from Wastewater Using Locally Sawdust," in *Proceeding of 1st International Conference of Southern Technical University/Iraq*, 2016, vol. 16, p. 17.

[18] I. H. Dakhil and A. S. Abbas, "Challenges and future directions in photoelectro-Fenton techniques: A comprehensive review of emerging applications and innovations," *Iraqi Journal of Chemical and Petroleum Engineering,* vol. 26, no. 3, pp. 63-83, 2025. https://doi.org/10.31699/IJCPE.2025.3.7

[19] A. Yerkebulan, I. Sapargali, S. Azat, Z. Toktarbay, and K. Kenes, "Performance Comparison of Agricultural Waste-Derived Carbonized Sorbents for Phenol Adsorption," *Engineered Science,* vol. 37, p. 1840, 2025. https://doi.org/10.30919/es1840

[20] I. H. Dakhil, G. F. Naser, and A. H. Ali, "Response Surface Modeling of Arsenic Adsorption by Modified Spent Tea Leaves," in *IOP Conference Series: Materials Science and Engineering*, 2021, vol. 1090, no. 1, p. 012129: IOP Publishing. https://doi/org/10.1088/1757-899X/1090/1/012129

[21] Y. Dehmani, T. Lamhasni, A. Mohsine, Y. Tahri, H.-s. Lee, H. Lgaz, A. A. Alrashdi, and S. Abouarnadasse, "Adsorption removal of phenol by oak wood charcoal activated carbon," *Biomass Conversion and Biorefinery,* vol. 14, no. 6, pp. 8015-8027, 2024. https://doi.org/10.1007/s13399-022-03036-5

[22] P. Limsuwan, J. Pongpai, D. Yiamsawas, W. Tanthapanichakoon, K. Maneeintr, J. Trakulmututa, A. Srikhaow, S. M. Smith, K. Sasaki, and C. Chuaicham, "Harnessing durian seed and shell waste-derived activated carbon for effective aqueous phenol removal," *Adsorption,* vol. 31, no. 2, p. 51, 2025. https://doi.org/10.1007/s10450-025-00606-7

[23] F. F. Zafar, B. Barati, D. Sanaei, S. Yousefzadeh, E. Ahmadi, M. Ansari, M. R. Ghalhari, H. Rasoulzadeh, X. Zheng, S. Wang, and H. Chen, "Application of Agricultural Waste-Based Activated Carbon for Antibiotic Removal in Wastewaters: A Comprehensive Review," *Water,* vol. 17, no. 8, 2025. https://doi.org/10.3390/w17081190

[24] I. H. Dakhil, "Recycling of Agriculture Wastes for Efficient Removal of Methyl Orange Dye Using Batch Adsorption Unit," in *IOP Conference Series: Materials Science and Engineering*, 2020, vol. 881, no. 1, p. 012186: IOP Publishing. https://doi.org/10.1088/1757-899X/881/1/012186

[25] C. A. Igwegbe, J. O. Ighalo, S. Ghosh, S. Ahmadi, and V. I. Ugonabo, "Pistachio (Pistacia vera) waste as adsorbent for wastewater treatment: a review," *Biomass Conversion and Biorefinery,* vol. 13, no. 10, pp. 8793-8811, 2023. https://doi.org/10.1007/s13399-021-01739-9

[26] L. A. d. S. de Jesus, R. L. B. Cabral, M. K. P. Ferreira, D. F. de Santana Souza, E. R. V. P. Galvão, R. B. Rios, and J. H. O. do Nascimento, "Evaluation of reduced graphene oxide from cotton waste as an efficient phenol adsorbent in aqueous media," *Environmental Science and Pollution Research,* vol. 32, no. 28, pp. 16881-16897, 2025. https://doi.org/10.1007/s11356-024-34708-6

[27] I. H. Dakhil, G. F. Naser, and A. H. Ali, "Assessment of Modified Rice Husks for Removal of Aniline in Batch Adsorption Process: Optimization and Isotherm Study," *Journal of Ecological Engineering,* vol. 22, no. 7, 2021. https://doi.org/10.12911/22998993/138900

[28] N. Yeasmen and V. Orsat, "Green extraction and characterization of leaves phenolic compounds: a comprehensive review," *Critical Reviews in Food Science and Nutrition,* vol. 63, no. 21, pp. 5155-5193, 2023. https://doi.org/10.1080/10408398.2021.2013771

[29] D. Seth, M. Athparia, A. Singh, D. Rathore, V. Venkatramanan, V. Channashettar, S. Prasad, S. Maddirala, S. Sevda, and R. Kataki,

"Sustainable environmental practices of tea waste—a comprehensive review," *Environmental Science and Pollution Research,* vol. 32, no. 12, pp. 7449-7467, 2025. https://doi.org/10.1007/s11356-023-30848-3

[30] N. A. Sagar, M. Pathak, R. Singh, E.-K. Seow, A. V. Chinchkar, and M. Sharma, "Chapter 74 - Usage of spent tea leaves: A new narrative," in *Tea in Health and Disease Prevention (Second Edition)*, V. R. Preedy and V. B. Patel, Eds.: Academic Press, 2025, pp. 863-877. https://doi.org/10.1016/B978-0-443-14158-4.00070-1

[31] M. Yanaka, S. Nagoya, and Y. Kawase, "A novel dynamic biosorption kinetic model based on reactions on the biosorbent surface for biosorption of heavy metal copper by non-living biomass waste tea leaves," *Environmental Surfaces and Interfaces,* vol. 3, pp. 90-102, 2025. https://doi.org/10.1016/j.esi.2025.02.001

[32] A. A. Alsarayreh, H. Q. Alzoubi, and M. N. Abbas, "Sustainable nickel removal from water by using waste tea leaves for eco-friendly water treatment," *Indian Chemical Engineer,* pp. 1-22, 2025. https://doi.org/10.1080/00194506.2025.2459833

[33] I. H. Dakhil and A. H. Ali, "Adsorption of methylene blue dye from industrial wastewater using activated carbon prepared from agriculture wastes," *Desalination and Water Treatment,* vol. 216, pp. 372-378, 2021. https://doi.org/10.5004/dwt.2021.26802

[34] A. Ouedrhiri, M. Ait Himi, B. Youbi, Y. Lghazi, J. Bahar, C. El Haimer, A. Aynaou, and I. Bimaghra, "Biochar material derived from natural waste with superior dye adsorption performance," *Materials Today: Proceedings,* vol. 66, pp. 259-267, 2022. https://doi.org/10.1016/j.matpr.2022.04.928

[35] A. A. Nassar, M. F. Mubarak, A. K. El-Sawaf, M. A. Zayed, and M. Hemdan, "Efficient lead ion removal from aqueous solutions for wastewater treatment using a novel cross-linked alginate-rice husk ash-graphene oxide-chitosan nanocomposite," *International Journal of Biological Macromolecules,* vol. 284, p. 137983, 2025. https://doi.org/10.1016/j.ijbiomac.2024.137983

[36] N. L. Bih, M. J. Rwiza, A. S. Ripanda, A. A. Mahamat, R. L. Machunda, and J. W. Choi, "Adsorption of phenol and methylene blue contaminants onto high-performance catalytic activated carbon from biomass residues," *Heliyon,* vol. 11, no. 1, 2025. https://doi.org/10.1016/j.heliyon.2024.e41150

[37] J. Lugo-Arias, S. B. Vargas, A. Maturana, J. González-Álvarez, E. Lugo-Arias, and H. Rico, "Nutrient Removal from Aqueous Solutions Using Biosorbents Derived from Rice and Corn Husk Residues: A Systematic Review from the Environmental Management Perspective," *Water*, vol. 16, no. 11, p. 1543. 2024 https://doi.org/10.3390/w16111543

[38] A. Chibani, C. Boucetta, M. A. N. Haddad, S. Merouani, S. Adjel, S. Merabet, H. Laidoudi, and C. Bougriou, "Effect of fin material type and reactor inclination angle on hydrogen adsorption process in large-scale activated carbon-based heat storage system," *Journal of Energy Storage,* vol. 98, p. 113091, 2024. https://doi.org/10.1016/j.est.2024.113091

[39] I. H. Dakhil, "Removal of phenol from industrial wastewater using sawdust," *Int. J. Eng. Sci,* vol. 3, no. 1, pp. 25-31, 2013.

[40] S. M. Anisuzzaman, A. Bono, D. Krishnaiah, and Y. Z. Tan, "A study on dynamic simulation of phenol adsorption in activated carbon packed bed column," *Journal of King Saud University - Engineering Sciences,* vol. 28, no. 1, pp. 47-55, 2024. https://doi.org/10.1016/j.jksues.2014.01.001

[41] D. O. Ozcan, M. C. Hendekci, and B. Ovez, "Enhancing the adsorption capacity of organic and inorganic pollutants onto impregnated olive stone derived activated carbon," *Heliyon,* vol. 10, no. 12, 2024. https://doi.org/10.1016/j.heliyon.2024.e32792

[42] O. C. Iheanacho, J. T. Nwabanne, C. C. Obi, and C. E. Onu, "Packed bed column adsorption of phenol onto corn cob activated carbon: linear and nonlinear kinetics modeling," *South African Journal of Chemical Engineering,* vol. 36, pp. 80-93, 2022. https://doi.org/10.1016/j.sajce.2021.02.003

[43] C. R. Girish and V. R. Murty, "Adsorption of Phenol from Aqueous Solution Using Lantana camara, Forest Waste: Packed Bed Studies and Prediction of Breakthrough Curves," *Environmental Processes,* vol. 2, no. 4, pp. 773-796, 2015. https://doi.org/10.1007/s40710-015-0117-z

[44] J. T. Nwabanne, O. C. Iheanacho, C. C. Obi, and C. E. Onu, "Linear and nonlinear kinetics analysis and adsorption characteristics of packed bed column for phenol removal using rice husk-activated carbon," *Applied Water Science,* vol. 12, no. 5, p. 91, 2022. https://doi.org/10.1007/s13201-022-01635-1

[45] M. Al Malki, A. Z. Yaser, M. A. A. M. Hamzah, M. A. A. Zaini, N. A. Latif, S. H. Hasmoni, and Z. A. Zakaria, "Date Palm Biochar and Date Palm Activated Carbon as Green Adsorbent—Synthesis and Application," *Current Pollution Reports,* vol. 9, no. 3, pp. 374-390, 2023. https://doi.org/10.1007/s40726-023-00275-6

[46] H. D. S. S. Karunarathne and B. M. W. P. K. Amarasinghe, "Fixed Bed Adsorption Column Studies for the Removal of Aqueous Phenol from Activated Carbon Prepared from Sugarcane Bagasse," *Energy Procedia,* vol. 34, pp. 83-90, 2023. https://doi.org/10.1016/j.egypro.2013.06.736

[47] E. Allahkarami, A. Dehghan Monfared, L. F. O. Silva, and G. L. Dotto, "Toward a mechanistic understanding of adsorption behavior of phenol onto a novel activated carbon composite," *Scientific Reports,* vol. 13, no. 1, p. 167, 2023. https://doi.org/10.1038/s41598-023-27507-5

نمذجة إمتزاز الفينول باستخدام الكاربون المنشط المُستخلص من أوراق الشاي المُستهلكة في عمود ذي طبقة مُحشوة

إحسان حبيب داخل [١]*، غازي فيصل ناصر[٢]، أحمد عبد الرزاق هادي[٣]، أحمد حسن علي[٤]
[١،٢،٤] قسم الهندسة الكيمياوية، كلية الهندسة، جامعة المثنى، العراق
[١] كلية الهندسة، جامعة العين العراقية، ذي قار، العراق
[٣] قسم العلوم، كلية التربية الأساسية، جامعة المثنى، المثنى، العراق
*البريد الإلكتروني: em2ihsan@mu.edu.iq

المستخلص

تهدف هذه الدراسة إلى بحث قدرة الكاربون المنشط المُستخلص من أوراق الشاي المُستهلكة (STLAC) كمادة مازة لإزالة الفينول من المياه الملوثة المُحاكاة في عمود ذي طبقة مُحشوة. تم تحضير STLAC عن طريق التنشيط الكيميائي من خلال التشريب بهيدروكسيد البوتاسيوم، متبوعًا بالتفحيم في ظل ظروف مُحكمة. تم توصيف الخصائص الفيزيائية والكيميائية للكاربون المنشط المُحضر. استُخدمت منهجية سطح الاستجابة مع تصميم المركب المركزي لنمذجة أربع معاملات تشغيلية: معدل الجريان، والتركيز الأولي للفينول، ارتفاع طبقة المادة الممتزة، ودرجة الحموضة. طُوّر نموذج رياضي لوصف العلاقة بين العوامل التشغيلية وكفاءة الإزالة. تُظهر النتائج قدرة عالية للكاربون المنشط STLAC في إزالة الفينول بكفاءة قصوى تبلغ ٩١,٩٢٪ عند عوامل التشغيل المثلى: معدل الجريان (١١,٤٦ مل/دقيقة)، والتركيز الأولي للفينول (١٩ ملغم/لتر)، وارتفاع طبقة المادة الممتزة (١٧,٨ سم)، ودرجة الحموضة (٦,٨). رُصدت نقطة الاختراق الأولى ونقطة التشبع عند ٣١ و٧٠ دقيقة على التوالي. أكدت دراسات التجديد فاعلية الكاربون المنشط STLAC لإعادة استخدامه في عملية الامتزاز بعد خمس دورات، بكفاءة تتجاوز ٧٥٪. يُظهر الكاربون المنشط STLAC أداءً تنافسيًا في إزالة الفينول، مُوفرًا مزايا من حيث الاستدامة والفعالية من حيث التكلفة. بحسب علمنا، تُعدّ هذه الدراسة الأولى من نوعها التي نمذجت بشكل منهجي إزالة الفينول باستخدام مادة STLAC في عمود ذي طبقة معبأة مستمرة، وذلك من خلال منهجية RSM-CCD، وتستخدم العوامل المُثلى لتحديد خصائص الاختراق. تُسلّط هذه الدراسة الضوء على إمكانية تحويل المخلفات الزراعية إلى منتجات ذات قيمة مضافة لتطبيقات المعالجة البيئية. تُبيّن هذه النتائج أن مادة STLAC مادة ماصة واعدة، منخفضة التكلفة، ومستدامة لإزالة الفينول من مياه الصرف الصناعي.